the FEBS Journal

Yeast protein glycation *in vivo* by methylglyoxal

Molecular modification of glycolytic enzymes and heat shock proteins

Ricardo A. Gomes[1], Hugo Vicente Miranda[1], Marta Sousa Silva[1], Gonçalo Graça[2], Ana V. Coelho[2,3], António E. Ferreira[1], Carlos Cordeiro[1] and Ana Ponces Freire[1]

1 Centro de Química e Bioquímica, Departamento de Química e Bioquímica, Faculdade de Ciências da Universidade de Lisboa, Portugal
2 Laboratório de Espectrometria de Massa do Instituto de Tecnologia Química e Biológica, Universidade Nova de Lisboa, Oeiras, Portugal
3 Departamento de Química da Universidade de Évora, Portugal

Keywords
kinetic modeling; methylglyoxal; peptide mass fingerprint; protein glycation; yeast

Correspondence
C. Cordeiro, Centro de Química e Bioquímica, Departamento de Química e Bioquímica, Faculdade de Ciências da Universidade de Lisboa, Edifício C8, Lisboa, Portugal
Fax: +351 217500088
Tel: +351 217500929
E-mail: cacordeiro@fc.ul.pt
Website: http://cqb.fc.ul.pt/enzimol/

(Received 28 June 2006, revised 14 September 2006, accepted 2 October 2006)

doi:10.1111/j.1742-4658.2006.05520.x

Protein glycation by methylglyoxal is a nonenzymatic post-translational modification whereby arginine and lysine side chains form a chemically heterogeneous group of advanced glycation end-products. Methylglyoxal-derived advanced glycation end-products are involved in pathologies such as diabetes and neurodegenerative diseases of the amyloid type. As methylglyoxal is produced nonenzymatically from dihydroxyacetone phosphate and D-glyceraldehyde 3-phosphate during glycolysis, its formation occurs in all living cells. Understanding methylglyoxal glycation in model systems will provide important clues regarding glycation prevention in higher organisms in the context of widespread human diseases. Using *Saccharomyces cerevisiae* cells with different glycation phenotypes and MALDI-TOF peptide mass fingerprints, we identified enolase 2 as the primary methylglyoxal glycation target in yeast. Two other glycolytic enzymes are also glycated, aldolase and phosphoglycerate mutase. Despite enolase's activity loss, in a glycation-dependent way, glycolytic flux and glycerol production remained unchanged. None of these enzymes has any effect on glycolytic flux, as evaluated by sensitivity analysis, showing that yeast glycolysis is a very robust metabolic pathway. Three heat shock proteins are also glycated, Hsp71/72 and Hsp26. For all glycated proteins, the nature and molecular location of some advanced glycation end-products were determined by MALDI-TOF. Yeast cells experienced selective pressure towards efficient use of D-glucose, with high methylglyoxal formation as a side effect. Glycation is a fact of life for these cells, and some glycolytic enzymes could be deployed to contain methylglyoxal that evades its enzymatic catabolism. Heat shock proteins may be involved in proteolytic processing (Hsp71/72) or protein salvaging (Hsp26).

Protein glycation is a post-translational modification whereby amino groups in arginine and lysine side chains react irreversibly with carbonyl molecules, forming advanced glycation end-products (AGEs). Glycation is equivalent to a point mutation, exerting profound effects on protein structure, stability and function. AGE formation in proteins is associated with the clinical complications of diabetes mellitus [1], cataracts [2], uremia [3], atherosclerosis [4] and age-related disorders [5]. Glycated proteins are present in β-amyloid deposits and τ deposits in Alzheimer's disease [6–8], in Lewy inclusion bodies of α-sinuclein in

Abbreviations
AGE, advanced glycation end-product; CEL, N^{ε}-(carboxyethyl)lysine; MAGE, methylglyoxal advanced glycation end-products.

Parkinson's disease [9], and in transthyretin amyloid deposits in familial amyloidotic polyneuropathy [10]. In all of these amyloid pathologies, β-sheet fibril structure and the presence of AGEs are common features, suggesting a possible role for glycation in amyloid formation and pathogenesis.

Methylglyoxal is the most significant glycation agent *in vivo*, being one of the most reactive dicarbonyl molecules in living cells. This compound is an unavoidable byproduct of glycolysis, arising from the nonenzymatic β-elimination reaction of the phosphate group of dihydroxyacetone phosphate and D-glyceraldehyde 3-phosphate [11]. Methylglyoxal reacts irreversibly with amino groups in lipids, nucleic acids and proteins, forming methylglyoxal advanced glycation end-products (MAGE) [12,13].

Argpyrimidine [N^{δ}-(5-hydroxy-4,6-dimethylpyrimidine-2-yl)-L-ornithine], hydroimidazolones [N^{δ}-(5-methyl-imidazolone-2-yl)-ornithine, isomers and oxidation products] and N^{δ}-(4-carboxy-4,6-dimethyl-5,6-dihydroxy-1,4,5,6-tetrahydropyrimidin-2-yl)ornithine are specific markers of protein glycation by methylglyoxal on arginine residues [13,14]. Methylglyoxal specifically forms N^{ε}-(carboxyethyl)lysine (CEL) and methylglyoxal–lysine dimer with lysine residues [15,16].

Understanding methylglyoxal catabolism and the identity of MAGE protein targets are of prime importance with regard to glycation prevention. In eukaryotic cells, two pathways are responsible for methylglyoxal detoxification. The first is formation of D-lactate by the glutathione-dependent glyoxalase system, comprising the enzymes glyoxalase I (lactoylglutathione methylglyoxal-lyase, EC 4.4.1.5) and glyoxalase II (hydroxyacylglutathione hydrolase, EC 3.1.2.6) [17]. The second is the production of 1,2-propanediol by NADPH-dependent aldose reductase (alditol:$NADP^+$ oxidoreductase, EC 1.1.1.21) [18]. In yeast, both pathways are equally important as antiglycation defences against protein glycation by methylglyoxal [19]. Given its high glycolytic flux and consequently high intracellular methylglyoxal concentration, yeast is highly susceptible to protein glycation, making it a suitable eukaryotic model organism with which to investigate this process *in vivo* [19]. Remarkably, only a few proteins appear to be extensively glycated, and yeast cells cope remarkably well with glycation *in vivo* by methylglyoxal, remaining viable and without apparent growth changes [19].

We identified the MAGE protein targets by peptide mass fingerprint and determined their nature and molecular location in the modified proteins. As some of these proteins are glycolytic enzymes, modeling and computer simulation was used to perform a sensitivity analysis of the glycation effects on glycolytic flux.

Results

Identification of glycated proteins

When nongrowing yeast cells are exposed to 250 mM D-glucose, protein glycation occurs after just 1 h in the reference strain BY4741 (Fig. 1). Against all expectations for a nonenzymatic process, glycation is primarily detectable in only one protein band of 52 kDa (Fig. 1B,C). Three more bands, of 70, 40 and 35 kDa appear after 3 h, with much less intensity (Fig. 1B,C). To identify the proteins, bands were excised from the BY4741 Coomassie-stained gel (Fig. 1A) and subjected to in-gel tryptic digestion. The resulting peptide mixtures were analyzed by MALDI-TOF for protein identification by peptide mass fingerprint. The 52 kDa protein was identified as enolase 2 (2-phospho-D-glycerate-hydrolyase, EC 4.2.1.11), as shown in Fig. 1E. To further confirm the identity of this major glycation target in yeast, a western blot analysis was performed, using a specific antibody against yeast enolase, with positive results (Fig. 1D). The 40 and 35 kDa proteins were identified as two other glycolytic enzymes (Fig. 1E), aldolase (D-fructose-1,6-bisphosphate-D-glyceraldehyde-3-phosphate-lyase, EC 4.1.2.13) and phosphoglycerate mutase (D-phosphoglycerate-2,3-phosphomutase, EC 5.4.2.1), respectively. The 70 kDa band was identified as a mixture of Hsp71 and Hsp72 (Fig. 1E).

The same nonglycated protein bands, i.e., proteins extracted in conditions in which glycation has not yet occurred (Fig. 1C, lane 1), were also identified as the same proteins. The corresponding protein bands from strains ΔGLO1 and ΔGRE3 were identified as the same proteins. Greater sequence coverage was obtained in peptide mass fingerprints of nonglycated proteins. This is to be expected, because glycated proteins contain modified lysine and arginine side chains, and therefore are less amenable to hydrolysis by trypsin and ionization. Moreover, due to the mass increase characteristic of an AGE, glycated peptides had no match in the databases and were therefore rejected. Nevertheless, this information can be exploited to identify the nature and molecular location of specific MAGE in glycated proteins.

Chemical nature and molecular location of MAGE in glycated proteins

In the peptide mass spectra of all glycated proteins, several new peaks appear that do not have predicted

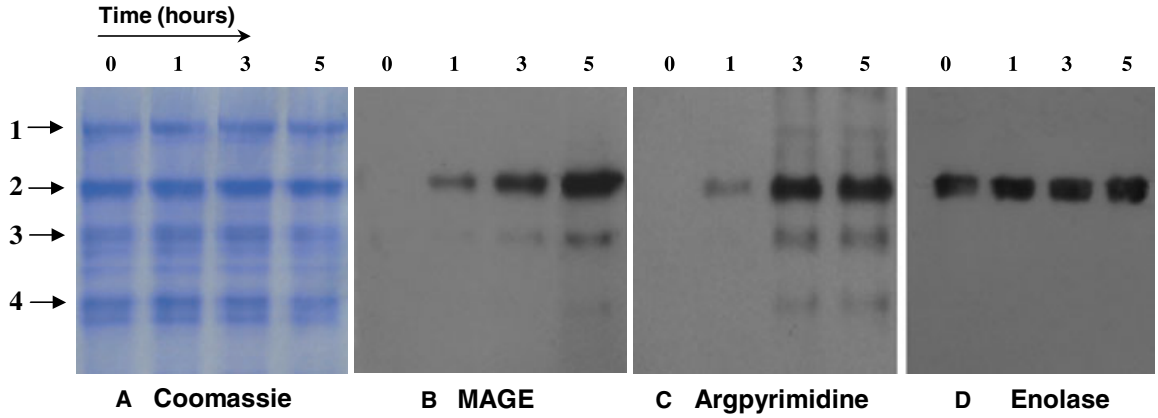

Band Nº	Swiss Prot Code	Identified Protein	Peptides matched	Mascot Score	Molecular Weight (Da)	Sequence Coverage
1	P10591	HSP71	22	176*	69 655	42 %
	P10592	HSP72	22		69 467	41 %
2	P00925	Enolase 2	10	128	46 811	27 %
3	P14540	Aldolase	7	81	39 750	32 %
4	P00950	Phosphoglycerate mutase	12	100*	26 394	47 %
	P15992	HSP26	10		23734	52 %

* Score for the protein mixture

E Protein identification

Fig. 1. The main methylglyoxal-modified proteins in yeast are the glycolytic enzymes enolase, aldolase and phosphoglycerate mutase and the heat shock proteins Hsp71/72 and Hsp26. Nongrowing BY4741 cells were incubated with 250 mM D-glucose to induce protein glycation *in vivo*. Samples, taken at the defined times, were analyzed for total protein, argpyrimidine, methylglyoxal advanced glycation end-products (MAGE) and enolase. Methylglyoxal-modified protein bands were excised and digested in gel with trypsin for protein identification by MALDI-TOF peptide mass fingerprint. The figure shows a representative result from a set of more than three independent experiments. Equal amounts of proteins were loaded per lane (30 μg). (A) Total protein Coomassie-stained gel. (B) MAGE detection by western blotting. (C) Argpyrimidine detection in intracellular soluble proteins, probed by western blotting with a specific antibody to argpyrimidine. Four major immunoreactive proteins were detected, the 52 kDa protein appearing as the main protein glycation target in yeast. (D) Enolase is the major glycation target in yeast. Total protein extract from strain BY4741, probed with antibody to enolase. The 52 kDa protein, which is highly modified by methylglyoxal, shows high immunoreactivity with antibody to enolase. (E) Identification of glycated proteins by MALDI-TOF peptide mass fingerprint. Criteria used for identification were significant homology scores achieved in MASCOT (53 for 95% confidence), a minimum of four peptides matched and a protein sequence coverage greater than 10%.

m/z values. These could be caused by the occurrence of miscleavage associated with defined mass increases of specific MAGE. To identify some probable glycated peptides and the specific MAGE present, we performed a theoretical digestion of the identified proteins, considering up to two trypsin miscleavages (PEPTIDEMASS, Expasy, http://www.expasy.ch/tools/peptide-mass.html) and added to the resulting peptide masses the mass increment due to a specific MAGE. Using this approach with enolase, we observed that several peptides do show a mass increment due to a specific MAGE. For example, the species at *m/z* 1723.9, present only in the peptide mass spectrum of glycated enolase, corresponds to peptide 409–422 with *m/z* 1669.9 plus 54 Da, a mass increase characteristic of a hydroimidazolone (Fig. 2A,B). This peptide has one miscleavage at R414, suggesting the presence of one hydroimidazolone in this position. Interestingly, the same peptide is present only in the digestion of nonglycated enolase at an *m/z* of 1670.0 (Fig. 2A). Moreover, the species at *m/z* 1741.9 corresponds to the enolase peptide of 1669.0 Da plus 72 Da due to CEL (Fig. 2B). The peptide at *m/z* 1669.0 has two lysine residues at positions 336 and 337. In this case, MS/MS data would indicate which residue is

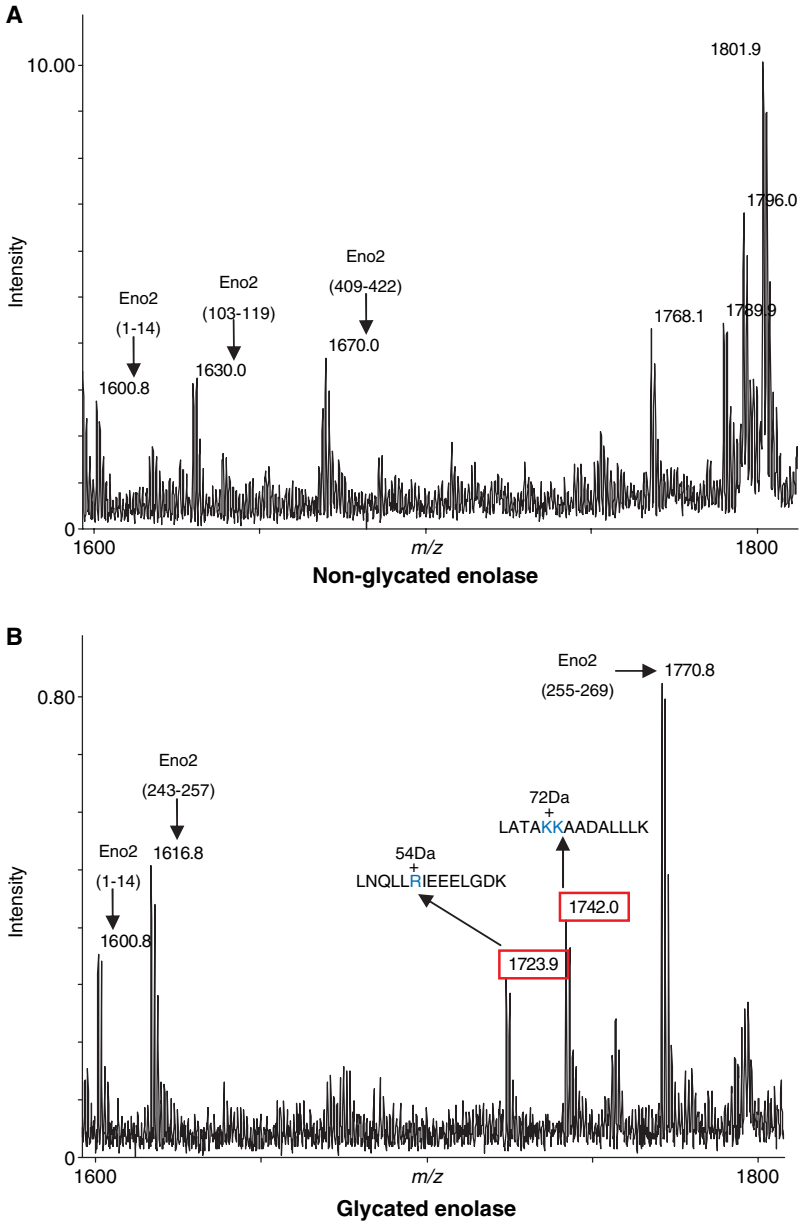

Fig. 2. Detection and molecular localization of methylglyoxal advanced glycation end-products (MAGE) in glycated enolase *in vivo*. The figure shows a section of a MALDI-TOF spectrum of tryptic digests of glycated and nonglycated enolase. (A) Mass spectrum of nonglycated enolase. (B) Same section of MALDI spectrum from glycated enolase. New peaks are detectable, and some of them represent glycated peptides (red). In this case, a hydroimidazolone (mass increase of 54 Da) in residue R414 and N^{ε}-(carboxyethyl)lysine (CEL) (mass increase of 72 Da) in residue K336 or K337 are observed.

modified. In the mass spectrum used to identify aldolase, the species with *m/z* 1082.5, which is absent in the non-glycated protein, corresponds to the aldolase peptide with a theoretical mass of 1002.5 Da plus 80 Da of argpyrimidine. Once more, the aldolase peptide of 1002.5 Da has one miscleavage in arginine residue 334. This method was applied to all mass spectra, and the results are shown in Table 1. We assumed that arginine or lysine residue modifications make these residues resistant to proteolysis by trypsin, and therefore that miscleavages associated with specific mass increases are due to glycation. These data further confirm, at the molecular level, that the identified proteins are indeed glycated *in vivo*. Considering that we have sequence coverage of the identified proteins of at most 50%, a significant fraction of glycated peptides was detected. This analysis shows that the most common MAGE *in vivo* are hydroimidazolones, followed by argpyrimidine, at about half the frequency, whereas CEL and tetrahydropyrimidine appear as minor modifications.

The refolding chaperone pathway in yeast glycation

Besides the identification of Hsp71 and Hsp72, another heat shock protein, Hsp26, was detected comigrating

Table 1. Identification and molecular location of methylglyoxal advanced glycation end-products (MAGE) in yeast glycated proteins. Glycated residues are shown in bold.

Identified protein	Observed mass (Da)	Theoretical peptide mass (Da)	Peptide sequence	Mass increase (Da)	MAGE	Glycated residue
Enolase	1723.92	1669.91	LNQLL**R**IEEELGDK (409–422)	54	Hydroimidazolone	R414
	1741.96	1669.03	IATAIE**KK**AADALLLK (330–345)	72	CEL	K336 or K337
	2196.08	2124.05	SVYDS**R**GNPTVEVELTTEK (9–27)	54	Hydroimidazolone	R14
Aldolase	1082.66	1002.54	VWV**R**EGEK (332–339)	80	Argpyrimidine	R335
Hsp71/72	1736.68	1664.92	IAS**K**NQLESIAYSLK (532–546)	72	CEL	K535
	2058.94	2004.92	**R**LIG**R**NFNDPEVQGDMK (69–85)[a]	54	Hydroimidazolone	R69 or R73

[a] Specific peptide from Hsp72.

with phosphoglycerate mutase (Fig. 1, band 4). In glycation conditions, more peptides from Hsp26 appear, whereas in nonglycated samples, only one or two are detected (Fig. 3). Thus, upon glycation, a larger number of Hsp26 molecules are found in the soluble protein fraction. As Hsp26 is mainly found as an insoluble 24-monomer complex that dissociates under stress conditions, its emergence in the soluble protein fraction is a sure sign of its activation [20]. Most peptides from phosphoglycerate mutase remain in the peptide mass spectrum from the glycated samples, as seen in Fig. 3 (47% sequence coverage). Hsp26 peptides lead to a sequence coverage of 52%. We then looked for the presence of glycated peptides from phosphoglycerate mutase and/or Hsp26. We observed that four peptides from phosphoglycerate mutase and one peptide from Hsp26 are glycated (Table 2).

Glycation effects on enolase activity and glycolysis

After identifying enolase as the primary glycation target, we investigated how its enzymatic activity was affected by glycation, in different yeast strains with distinct glycation phenotypes [19]. Strains BY4741, ΔGLO1 and ΔGRE3, with different glycation levels, were challenged with 250 mM D-glucose, and enolase activity was determined *in situ*.

The YEpGRE3 transformant, overexpressing aldose reductase, was used as a nonglycated control [19]. YEpGRE3 cells are better protected against methylglyoxal-derived glycation, due to the increased GRE3 expression and increased aldose reductase activity. In this strain, glycation was only observed after 5 h, contrasting with strains BY4741, ΔGLO1 and ΔGRE3, where it was detected after just 1 h, with increasing respective intensities (Fig. 4A). Strains with glycated enolase (BY4741, ΔGLO1 and ΔGRE3) showed a decrease of this enzyme activity, compared to the initial value, whereas the YEpGRE3 transformant, without glycated enolase, did not show enolase activity changes (Fig. 4B). This result indicates that glycation leads to a decrease of enolase activity. Consistent with the observation that glycation increases with time (Fig. 4A), after 2 h, *in situ* enolase activity was lower than after 1 h for all strains analyzed, except for the control YEpGRE3 transformant, in which enolase activity remained unchanged (Fig. 4B).

The reference strain BY4741 displayed the lowest decrease of enolase activity (5% and 10% after 1 h and 2 h, respectively), whereas strains ΔGLO1 and ΔGRE3 suffered a larger decrease of enzyme activity (Fig. 4B). These results are in agreement with the corresponding glycation phenotypes. After 1 h, ΔGRE3 glycated enolase shows a 16% decrease of enzyme activity, higher than the 8% decrease observed in the ΔGLO1 strain.

Given the decrease in enolase activity caused by glycation, a study of D-glucose metabolism in these cells was performed (Fig. 5A). For this purpose, D-glucose, ethanol and glycerol were measured at different times, after incubation with 250 mM D-glucose. As three glycolytic enzymes are glycated, we expected that the glycolytic flux, measured by D-glucose consumption and ethanol formation, might be affected. Strikingly, no major differences were observed in the glycolytic flux of strains BY4741, ΔGLO1 and ΔGRE3 (Fig. 5B). Glycolytic flux remained unchanged even in strains with deficiencies in methylglyoxal catabolism, showing higher enolase glycation and consequent inactivation.

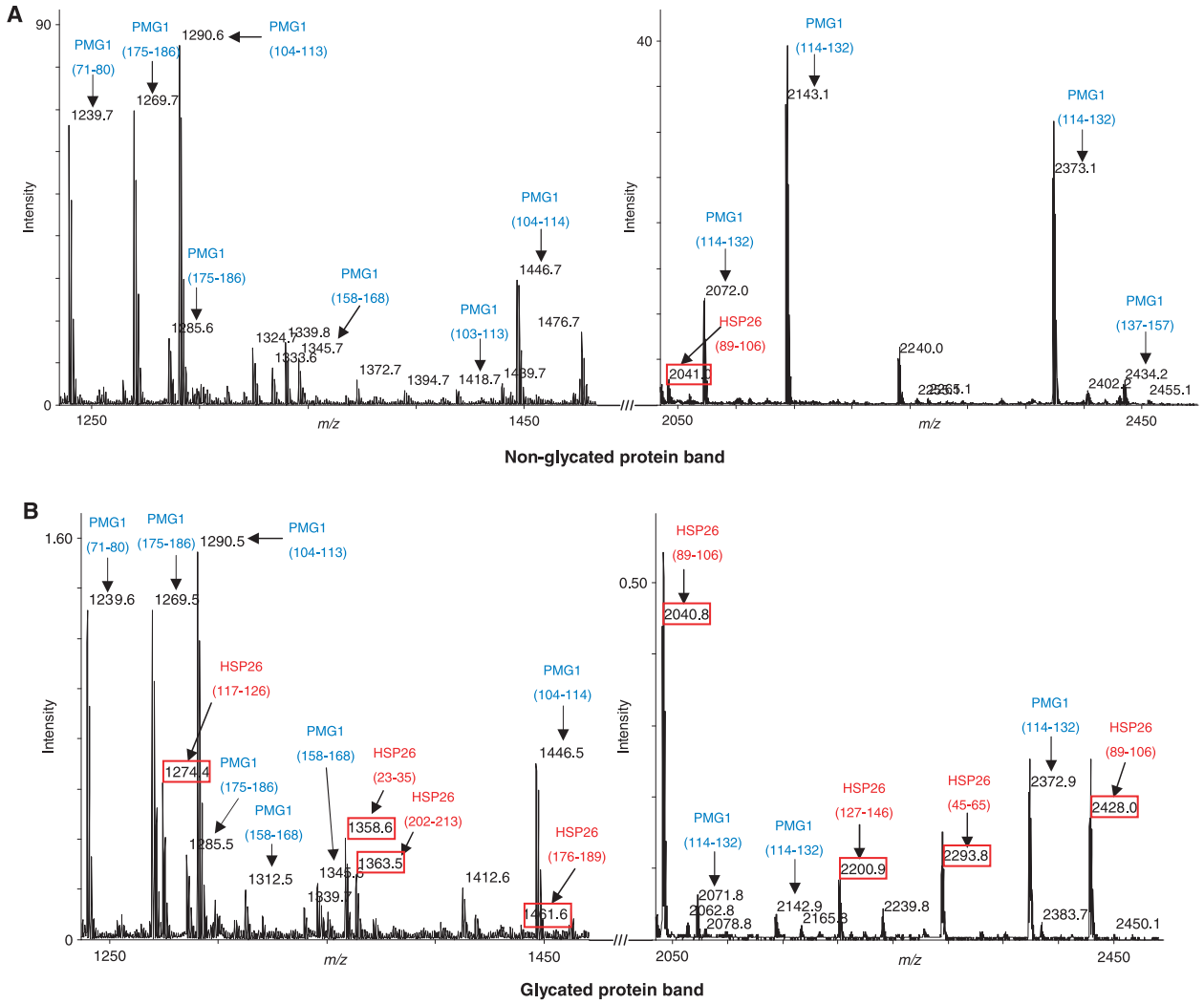

Fig. 3. Detection of Hsp26 upon glycation. (A) MALDI-TOF spectra of tryptic digestion of the nonglycated protein band 4, mainly showing peptides from phosphoglycerate mutase and one peptide, with low intensity, from Hsp26 (Fig. 1). In glycation conditions, more peptides from Hsp26, with greater intensity, appear. These data suggest that the amount of Hsp26 in the soluble protein fraction increases upon glycation.

Table 2. Analysis of the comigrating proteins phosphoglycerate mutase and Hsp26 under glycation conditions; identification and molecular location of methylglyoxal advanced glycation end-products (MAGE). Glycated residues are shown in bold.

Identified proteins	Observed mass (Da)	Theoretical peptide mass (Da)	Peptide sequence	Mass increase (Da)	MAGE	Glycated residue
Phosphoglycerate mutase	1320.48	1239.69	AD**R**LWIPVNR (71–80)	80	Argpyrimidine	R73
	1500.55	1446.71	FGEEKFNTY**R**R (104–114)	54	Hydroimidazolone	R113
	1574.58	1429.72	LNE**R**HYGDLQGK (84–95)	144	Tetrahydropyrimidine	R87
	2360.94	2280.28	DLLSGKTVMIAAHGNSL**R**GLVK (169–190)	80	Argpyrimidine	R186
Hsp26	1412.63	1358.75	LLGEGGL**R**GYAPR (23–35)	54	Hydroimidazolone	R30

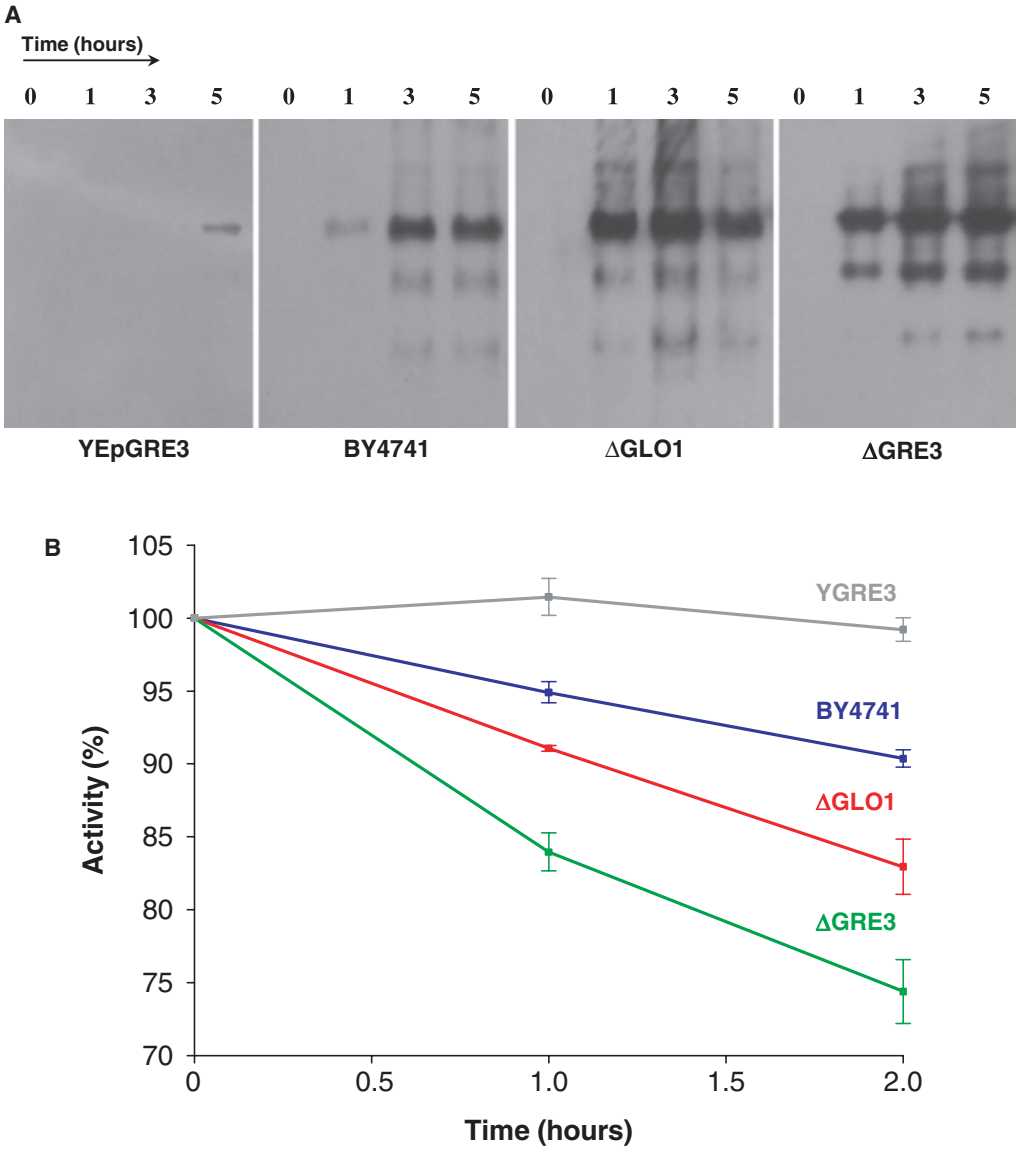

Fig. 4. *In vivo* glycation of enolase causes a decrease of its enzyme activity, directly related to glycation levels. Cells from different yeast strains, incubated with 250 mM D-glucose, were sampled at the times indicated. Glycated proteins were detected by western blotting using a specific anti-argpyrimidine Ig, and enzyme activity was determined *in situ*. (A) Time course of argpyrimidine formation in the YEpGRE3 transformant, BY4741, ΔGLO1 and ΔGRE3 strains. As a result of aldose reductase overexpression, YEpGRE3 only shows an argpyrimidine-modified protein band after 5 h. Strains with deficiencies in methylglyoxal catabolism (ΔGLO1 and ΔGRE3) have higher methylglyoxal concentrations and therefore higher levels of glycation [19]. It is noteworthy that glycation increases with time. Representative immunoblots from a set of more than three experiments are shown. Equal amounts of proteins were loaded per lane (30 μg). (B) *In situ* enolase activity in all studied strains, at different incubation times. Percentage activity is shown relative to time zero. A decrease of enolase activity is only observed in strains with glycated enolase, and this decrease is related to glycation levels. Data are averages from three independent experiments ± SDE.

As glycolysis leads unavoidably to methylglyoxal formation, which modifies three glycolytic enzymes, D-glucose metabolism could be diverted to glycerol synthesis. Increasing glycerol formation could diminish the methylglyoxal concentration, because the triose phosphate pool is reduced due to its conversion to glycerol 3-phosphate. However, no significant differences were observed in glycerol concentration between those strains (Fig. 5B).

These results indicate that glycation *in vivo* of enolase and other glycolytic enzymes, with corresponding loss of enzyme activity, does not affect glycolytic flux.

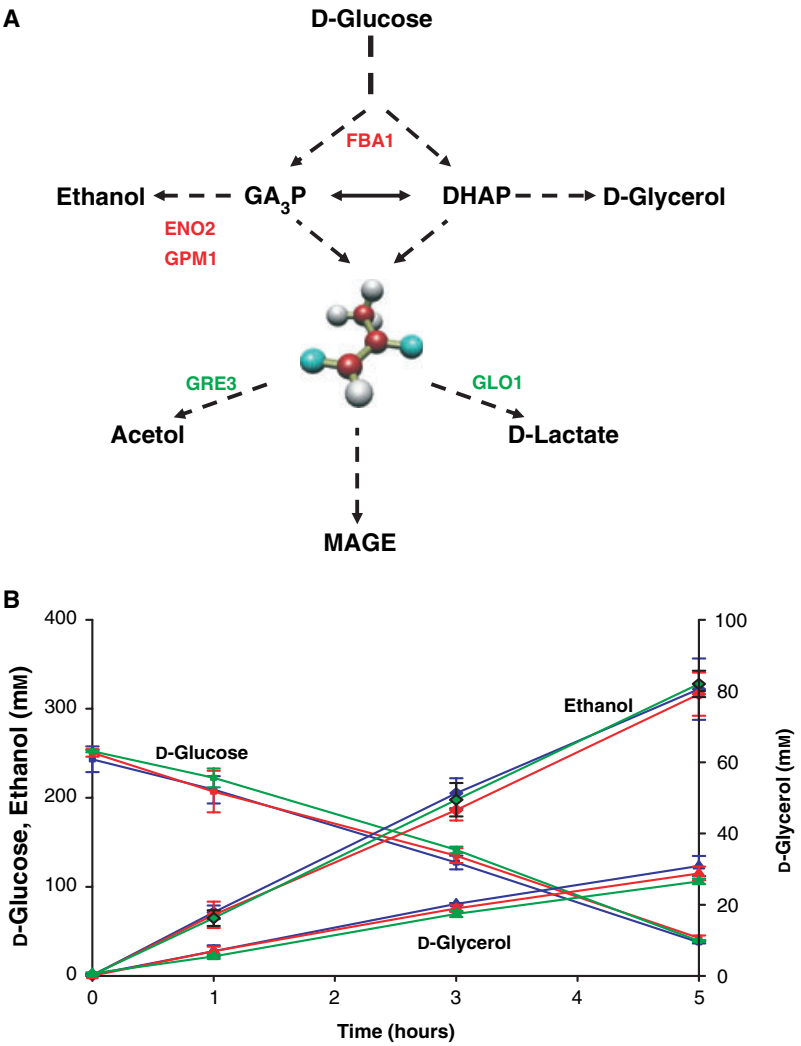

Fig. 5. Glycolysis, methylglyoxal metabolism and glycated proteins in yeast. (A) The well-known glycolytic pathway forms methylglyoxal as a nonenzymatic and unavoidable byproduct. The triose phosphates are chemically unstable and suffer an irreversible β-elimination reaction of the phosphate group, forming the most powerful glycation agent *in vivo*, methylglyoxal. The main catabolic routes for methylglyoxal are the NADPH-dependent aldose reductase and the glutathione-dependent glyoxalase pathway. Together, aldose reductase and glyoxalase I (green) are essential to maintain a low methylglyoxal steady-state concentration. Once formed, methylglyoxal has the potential to irreversibly modify just about any protein. However, in yeast, only one protein appears as a major target, enolase 2, followed by aldolase and phosphoglycerate mutase (red). (B) Glycolysis and glycerol metabolism are unchanged by glycation. Energy metabolism appears to be unaffected, even when three glycolytic enzymes are glycated and the major glycation target, enolase 2, shows an activity loss of 20%. The strains analyzed were BY4741 (blue), ΔGRE3 (green) and ΔGLO1 (red). Data shown are averages from three independent experiments ± SD.

To further investigate why this is so, a sensitivity analysis using modeling and computer simulation was performed.

Sensitivity analysis of glycation effects on glycolysis

The effect of changes in the activity of the main glycation targets, enolase, aldolase and phosphoglycerate mutase, on the glycolytic flux, as predicted by modeling and computer simulation, is shown in Fig. 6. Aldolase and phosphoglycerate mutase had no effect on glycolytic flux, even when their activities had decreased to 1% of their reference activities (Fig. 6B,C). Glycolytic flux was more sensitive to enolase activity: a reduction of approximately 50% in ethanol formation predicted a reduction of enolase activity to 5% (Fig. 4A). However, a simultaneous decrease of aldolase, enolase and phosphoglycerate mutase activities to 70% of their reference activities caused a glycolytic flux decrease of less than 0.02%.

According to these results, the decrease in enolase activity caused by glycation (between 5 and 25% *in vivo*) should have no effect on glycolytic flux. This is in agreement with our experimental results, where no differences in D-glucose consumption and ethanol formation were observed among strains BY4741, ΔGLO1 and ΔGRE3 (Fig. 5B).

Even the simultaneous glycation of these three enzymes, each one losing about one-third of its reference activity, would not cause any noticeable decrease of glycolytic flux.

As glycolysis leads unavoidably to methylglyoxal formation, and glycation selectively modifies glycolytic enzymes, causing activity loss, changes in glycerol metabolism might occur. As a result of a slight decrease in the triose phosphate pool (data not shown) methylglyoxal concentration is indeed sensitive to

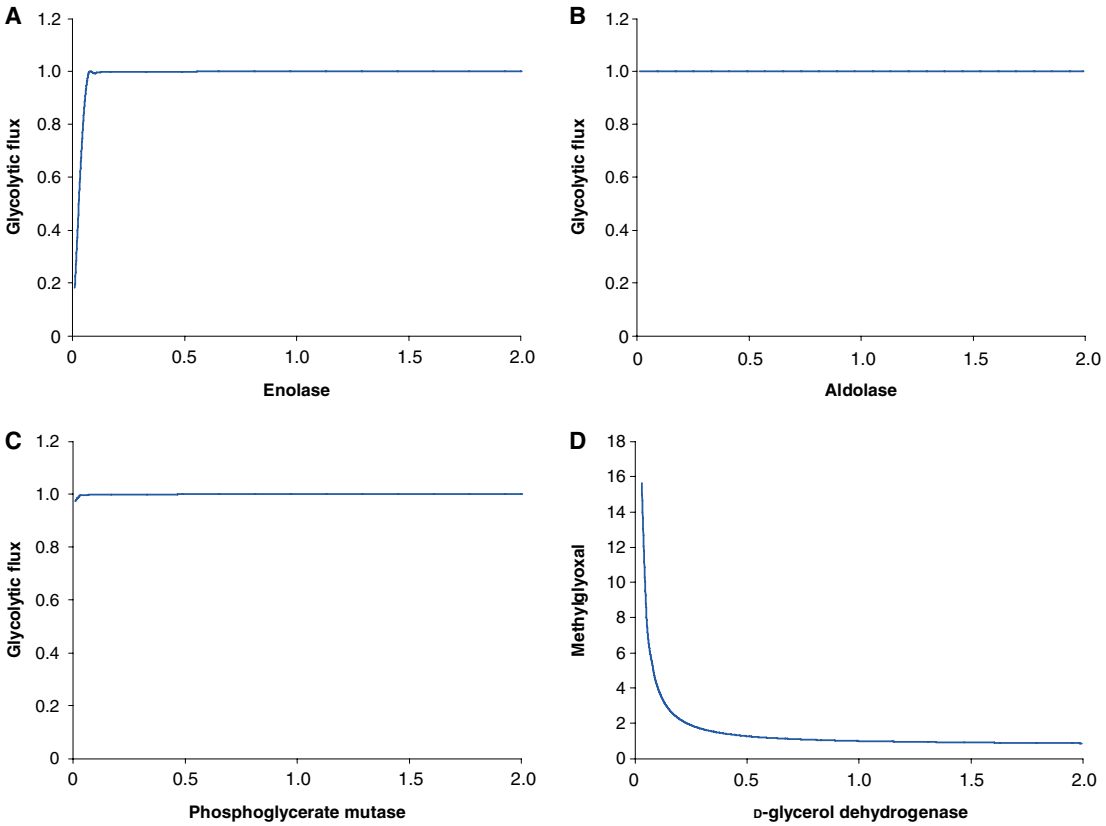

Fig. 6. Sensitivity analysis of glycation effects on glycolytic flux by modeling and computer simulation. Single, finite parameter changes (between zero-fold and two-fold) around the reference steady state were performed. All values are fold variations relative to the reference state (normalized values). System parameters were: (A) enolase activity; (B) aldolase activity; and (C) phosphoglycerate mutase activity. The effect of glycerol-3-phosphate dehydrogenase activity on methylglyoxal steady-state concentration (D) was also studied. Except for extreme changes (95–99% activity loss), the glycated glycolytic enzymes enolase, aldolase and phosphoglycerate mutase have no effects on glycolytic flux. Consistent with our experimental results, a decrease in enolase activity due to glycation has no effects on ethanol formation and D-glucose consumption.

changes in glycerol-3-phosphate dehydrogenase (EC 1.1.99.5) activity (Fig. 6D). An increase in glycerol-3-phosphate dehydrogenase activity by up to five-fold does not lead to a significant decrease in the steady-state concentrations of methylglyoxal and triose phosphates. Therefore, simulation of glycerol formation cannot lead to a decrease in methylglyoxal concentration. These predictions are consistent with the observations that glycerol metabolism is quantitatively identical in the three strains studied.

Discussion

Yeast cells have evolved to use D-glucose efficiently; for this, they have a very high glycolytic flux and consequently an unavoidably high methylglyoxal production rate. Therefore, throughout evolution, defence mechanisms have developed to protect these cells against glycation. Understanding these mechanisms will provide important clues regarding glycation prevention in higher organisms. Nerve cells show a high rate of glycolysis, and several neurodegenerative diseases, such as Alzheimer's disease and Parkinson's disease, are related to higher AGE formation [8,9]. Tumor cells also show a high dependence on glycolysis, the Warburg effect [21]. In these cells, expression of glyoxalase I is increased [22,23], suggesting that an increase in methylglyoxal and AGE formation also occurs.

In yeast, protein glycation is a nonrandom process for which specific protein targets exist. Even though several proteins are observed in a Coomassie-stained gel, only one is highly modified by methylglyoxal. Three more protein bands appear to be slightly modified at a later time, as judged by the western blotting analysis. This is an unexpected observation, because, as glycation is a nonenzymatic process, all proteins are putative targets. We identified the four major glycation targets as the glycolytic enzymes enolase, aldolase and phosphoglycerate

mutase and the heat shock proteins Hsp71/72 by MALDI-TOF peptide mass fingerprint. Under glycation conditions, Hsp26 becomes detectable in the soluble protein fraction. Of these proteins, enolase 2 is clearly the primary and most relevant glycation target in yeast. Glycation introduces miscleaveges and defined mass increases in the observable peptides produced by trypsin hydrolysis. Therefore, we analyzed the peptide masses, looking for miscleaveges associated with specific mass increases caused by the presence of MAGE in peptides containing one lysine or arginine residue. With this approach, we confirmed at the molecular level that the identified proteins are indeed glycated *in vivo* by methylglyoxal, and in some cases, the molecular position assignment of the specific MAGE was made. In enolase 2, the modified lysines (CEL) are probably those with the highest solvent accessibility (Fig. 7). In contrast, hydroimidazolone-modified arginines were only found in an arginine-rich crevice, located at the enolase 2 dimer interface (Fig. 7). This arginine-rich cave could work as a cage for free methylglyoxal.

Glycation of enolase *in vivo* causes a decrease of its activity, directly related to methylglyoxal modification. Strains ΔGLO1 and ΔGRE3, with deficiencies in methylglyoxal catabolism and therefore higher levels of glycation [19], cause a larger decrease in enolase activity. The YEpGRE3 transformant, overexpressing aldose reductase, does not show glycation, and no decrease of enolase activity occurs. However, in all strains analyzed, D-glucose consumption and ethanol formation rates were unchanged even when glycated enolase was present. Glycerol synthesis, an alternative branch point of glycolysis, remains unchanged. These results show that glycolytic flux is not affected, despite the decreased activity of enolase in all strains in which glycation occurs.

Sensitivity analysis, by modeling and computer simulation, was used to assess the effects of each glycated glycolytic enzyme on glycolysis. For enolase, glycolytic flux is affected only when its activity decreases to 5% of its reference activity value. This is almost equivalent to an enolase null mutant yeast strain, which is not viable. The other two major glycation targets (aldolase and phosphoglycerate mutase) have virtually no effect on glycolytic flux, in good agreement with our experimental observations.

As glycation is a nonenzymatic process, it is quite intriguing that it is targeted to specific proteins, the functional aspects involved being as yet unknown. As methylglyoxal arises from glycolysis, perhaps these proteins are closer to the location of methylglyoxal formation than others, and the methylglyoxal concentration is higher near these proteins. However, other glycolytic enzymes located more closely to methylglyoxal formation, such as triose phosphate isomerase and D-glyceraldehyde-3-phosphate dehydrogenase, are not glycated.

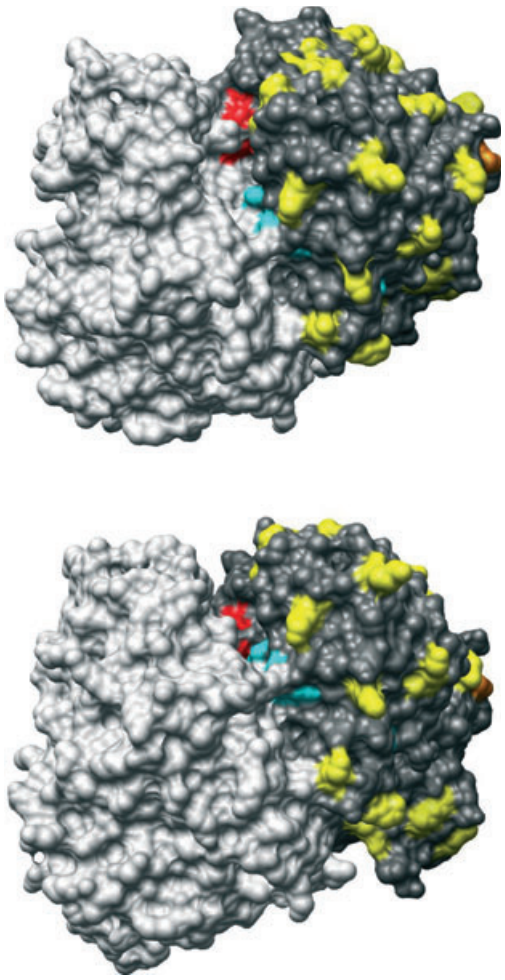

Fig. 7. Surface landscape of dimeric yeast enolase, showing solvent-exposed lysine (yellow) and arginine (cyan) residues. For greater clarity, the surface of one of the subunits is shown in light gray. Two views of the same molecule are shown, rotated clockwise by 180° along the molecule's horizontal axis. According to MALDI-TOF analysis, N^{ε}-(carboxyethyl)lysine (CEL) (orange) is located at K336 or K337. K336 (47% solvent accessibility) is by far the most solvent-accessible lysine in both subunits, and is likely to be glycated. Hydroimidazolones (red) were found only in R14 and R414, located in an arginine-rich cleft, deeply recessed, but solvent accessible, at the interface of the two enolase subunits. The E20-R414 ion pair is essential for dimer stability. Its disruption upon glycation will lead to dimer dissociation into inactive monomers, thus explaining at a molecular level the glycation-dependent enolase inactivation. This arginine-rich cave should provide highly favored reaction conditions for methylglyoxal advanced glycation end-product (MAGE) formation, therefore sequestering methylglyoxal in an arginine cage. Sequence coverage by MALDI-TOF peptide mass fingerprint is highly representative, at 27%. Confirmed nonglycated residues are not shown.

Of the identified glycated proteins, aldolase is the only enzyme directly related to methylglyoxal formation, and it only shows comparatively low glycation. Enolase, one of the most abundant proteins in yeast, could be associated with different glycolytic enzymes, and therefore the methylglyoxal concentration near this enzyme might be much higher than in the rest of the cell. Interestingly, in mammal cells, pure ββ-enolase binds with high affinity to the glycolytic enzymes aldolase and phosphoglycerate mutase (the other two main glycation targets in yeast) and also to pyruvate kinase [24].

Protein concentration *in vivo* and arginine content might be other important parameters for protein glycation. Enolase is indeed one of the most abundant cell proteins. However, the differences between the arginine content of this enzyme and those of most yeast glycolytic enzymes (containing between eight and 13 arginine residues) do not explain this specific glycation. Moreover, phosphofructokinase (with 49 arginine residues) and pyruvate kinase (with 29 arginine residues) are not glycated. It is possible that arginine residues in enolase are more accessible for the reaction with methylglyoxal than they are in other proteins. This highlights the importance of the reactivity of individual proteins towards methylglyoxal, beyond a simple consideration of protein amount or number of amino groups. *In vivo*, this reactivity could depend not only on the arginine and lysine contents, or protein and glycation agent concentrations, but also on the spatial location of arginine residues in a folded protein. It is not known whether this spatial location determines glycation specificity, but it is conceivable that the 14 arginine residues in enolase are more reactive towards methylglyoxal than are the 49 arginine residues of phosphofructokinase. As demonstrated by Speer *et al.*, the reactivity of arginine peptides with methylglyoxal varies widely, due to the local chemical environment of the respective arginine residue [25]. In the case of enolase 2, the glycated lysines are those with the highest solvent accessibility (Fig. 7). Whereas glycated lysines are at the exposed surface of the protein, glycated arginines are located in an arginine-rich deep cleft, accessible to the solvent, at the interface between the two subunits (Fig. 7). Some of these arginines are involved in ion pairs that contribute to enolase 2 dimer stability. One of these ion pairs, E20-R414 [26], is disrupted by R414 glycation. Replacing arginines with hydroimidazolones will disrupt electrostatic interactions that stabilize the enolase 2 dimer, leading to its dissociation and the consequent formation of inactive monomers. This molecular hypothesis for glycation-dependent enolase 2 inactivation, albeit highly plausible, requires further research.

It has been shown that cells can prevent AGE formation only until antiglycation defences are overcome [19]. In these conditions, spontaneous protein glycation may be relevant to lower methylglyoxal concentrations. Enolase could indeed function as a methylglyoxal scavenger, preventing changes in the biochemical functionalities of other proteins. Being one of the most abundant proteins in cells, enolase is a good candidate for this role, as glycation of this protein would only have a limited impact on cell physiology. Indeed, our results show that, although glycation leads to a decrease of enolase activity, no changes have been detected in glycolytic flux, even in the mutant strains ΔGLO1 and ΔGRE3, which show higher levels of glycation. It is noteworthy that the expression of ENO2 is induced up to 20-fold after the addition of glucose to yeast cells grown with ethanol as carbon source [27], whereas by modeling and computer simulation, a corresponding 20-fold increase of this enzyme's activity would have no effect at all on glycolytic flux. Enolase may thus play other roles, besides being a glycolytic enzyme.

It was predicted that MAGE would be present in approximately 3–13% of cellular proteins [28]. This is expected to have significant effects on protein structure and function, mainly by unfolding and aggregation [28]. In the presence of denatured proteins, cells activate several pathways responsible for their recovery, preventing the detrimental effects of protein aggregation. In yeast, Hsp104 facilitates disaggregation and reactivates aggregated proteins with assistance from Hsp71 (Ssa1) and Hsp40 (Ydj1) [29]. Recent data show that the small heat shock protein Hsp26 also participates in the recovery of misfolded proteins, by rendering aggregates more accessible to Hsp104/Hsp71/Hsp40 action [29]. The presence of Hsp26 in glycation conditions suggests that there is activation of the refolding chaperone pathway. Moreover, glycation also affects Hsp71/72, another component of this chaperone pathway, and Hsp26 is also glycated *in vivo*. In mammal cells, the major glycation target *in vivo* is Hsp27, a protein that plays an important role in apoptosis and actin polymerization [30,31]. In stressed cells, increased levels of Hsp27 facilitate the repair or destruction of damaged proteins, thus promoting cell recovery. It has been shown that specific methylglyoxal modification of Hsp27 improves its chaperone activity [30,32]. Thus, glycation and/or activation of these specialized proteins (Hsp71/72 and Hsp26) could be of physiologic importance in the cell response to glycation.

As glycolysis is a biochemical pathway that evolved under ancient anaerobic terrestrial conditions, it is possible that specialized proteins present in higher organisms are derived from glycolytic enzymes. This could be a

critical evolutionary parameter for cells with high glycolytic fluxes and high intracellular methylglyoxal concentrations. Another important process is the refolding pathway, through which stress-unfolded proteins might be salvaged in significant amounts, instead of simply being processed by proteolytic pathways.

Experimental procedures

Reagents

Peptone, yeast extract, agar and yeast nitrogen base (YNB) were obtained from Difco (San Jose, CA, USA), and D-glucose (microbiology grade), KCl, NaCl, $MgSO_4$, methanol and bromophenol blue were obtained from Merck (Rahway, NJ, USA). Coomassie Brilliant Blue G, Ponceau S, phenylmethylsulfonyl fluoride, glass beads (452–600 μm), adenine, uracil, L-methionine, L-histidine, L-leucine, L-tryptophan, Mes, 3-phosphoglycerate, formic acid, ammonium hydrogencarbonate, dithiothreitol and iodoacetamide were obtained from Sigma (St Louis, MO, USA). KH_2PO_4 was obtained from Fluka (St Louis, MO, USA), digitonin was obtained from CalBiochem (San Diego, CA, USA), and EDTA was obtained from BDH Chemicals Ltd (Poole, UK). Tris, SDS 20% (w/v) and glycine were obtained from Bio-Rad (Hercules, CA, USA). Modified trypsin was obtained form Promega (Madison, WI, USA); GELoader tips were obtained from Eppendorf (Hamburg, Germany); trifluoroacetic acid and HPLC-grade acetonitrile were obtained from Riedel de Häen (Seelze, Germany); type I water was obtained in a Millipore (Billerica, MA, USA) Milli-Q system; POROS 10 R2 reversed-phase chromatography medium was obtained from PerSeptive Biosystems (Framingham, MA, USA); α-cyano-4-hydroxycinnamic acid and PepMix1 (mixture of peptide standards) were obtained from LaserBiolabs (Framingham, MA, USA).

Yeast strains and culture conditions

Saccharomyces cerevisiae strains, Euroscarf collection (Frankfurt, Germany), were: BY4741 (genotype BY4741 *MATa*; *his3*Δ1; *leu2Δ0*; *met15Δ0*; *ura3Δ0*), ΔGLO1 (isogenic to BY4741 with YML004c::KanMX4) and ΔGRE3 (isogenic to BY4741 with YHR104w::KanMX4). The YEpGRE3 transformant [33] was kindly provided by J Prieto (Department. Biotech., Instituto de Agroquimica y Tecnologia de los Alimentos, Valencia, Spain). Strains were kept in YPGlu (0.5% w/v yeast extract, 1% w/v peptone and 2% w/v D-glucose) agar slopes (2% w/v agar) at 4 °C and cultured in liquid YPGlu medium or YNB (0.67% w/v yeast nitrogen base, 2% w/v D-glucose and 0.025% w/v L-methionine, L-histidine, L-leucine and uracil). The YEpGRE3 transformant was cultured in minimal YNB medium without L-leucine (0.67% w/v yeast nitrogen base, 2% w/v D-glucose, 0.02% w/v adenine, L-histidine, L-tryptophan and uracil).

Glycation experiments

Cells were harvested at the end of the exponential phase, washed twice in type II water, suspended at a concentration of 5.2×10^8 in 0.1 M Mes/NaOH (pH 6.5) with 250 mM D-glucose, and incubated at 160 r.p.m. and at 30 °C in an orbital shaker (Infors HT, Bottmingen, Switzerland). Samples were taken at defined times for enzyme activity assays, metabolite measurement and protein glycation analysis by western blot.

Analysis of protein glycation by western blot

Total yeast protein extraction was performed by glass bead lysis as previously described [19]. Protein concentration was determined using the Bio-Rad Bradford assay kit. Proteins (30 μg protein per lane) were separated by SDS/PAGE in a Mini-protean 3 system (Bio-Rad), using a 12% polyacrylamide separation gel and a 6% polyacrylamide stacking gel. Proteins were transferred to poly(vinylidene difluoride) membranes (Hybond-P; Amersham Pharmacia Biotech, Uppsala, Sweden), using the Mini Trans-Blot system (Bio-Rad). Transfer was performed with 39 mM glycine, 48 mM Tris, 0.0375% (w/v) SDS, and 20% (v/v) methanol. Prestained standard proteins (Bio-Rad) were also loaded onto the gel. Total proteins were stained with Ponceau S solution [0.5% (w/v) Ponceau S in 1% (v/v) glacial acetic acid] to confirm the amount of protein transferred. The membrane was blocked overnight at 4 °C in 1% (v/v) blocking solution in TBS (50 mM Tris and 150 mM NaCl, pH 7.5). For argpyrimidine detection, the blots were probed with monoclonal antibody to argpyrimidine, a kind gift from K. Uchida (Laboratory of Food and Biodynamics, Nagoya University Graduate School of Bioagricultural Sciences, Japan). Other methylglyoxal-derived AGEs were probed with a polyclonal anti-methylglyoxal modification, kindly provided by R. Nagaraj, Case Western University, Cleveland, OH, USA. An antibody to enolase, a kind gift from S. H. Park (Department of Microbiology, Chungnam National University, Korea), was used to identify this protein in membranes. Washes, secondary antibody and detection procedures were performed using the BM Chemiluminescence Western Blotting Kit (Roche, Indianapolis, IN, USA), following the manufacturer's instructions. Each immunoblot was repeated at least three times in independent experiments.

Protein identification by peptide mass fingerprint

Protein bands were excised and polypeptides subjected to reduction, alkylation and digestion with sequencing-grade modified trypsin in gel according to the method of Pandey

et al. [34]. Sample peptides were assayed for peptide mass fingerprint in a Voyager-DE STR MALDI-TOF mass spectrometer (Applied Biosystems, Foster City, CA, USA). The peptide mixture was purified and concentrated by R2 pore microcolumns [35] and eluted directly to the MALDI plate with 0.8 μL of recrystallized matrix α-cyano-4-hydroxycinnamic (10 $mg{\cdot}mL^{-1}$) prepared in 70% (v/v) acetonitrile with 0.1% (v/v) trifluoroacetic acid. The mixture was allowed to air dry (dried droplet method). Monoisotopic peptide masses were used to search for homologies and protein identification with PEPTIDE MASS FINGERPRINT of MASCOT (http://www.matrixscience.com). Searches were performed in the MSDB database. A mass accuracy of 50–100 p.p.m. was used for external calibrations, and Cys carbamidomethylation and Met oxidation were used as fixed and variable amino acid modifications, respectively. Criteria used to accept the identification were significant homology scores achieved in MASCOT (53 for 95% confidence) and a minimum of four peptides matched with a protein sequence coverage greater than 10%.

Metabolite assay

All metabolites were measured in the extracellular medium after removing the cells by centrifugation (5200 ***g***, 3 min, Eppendorf 5480 R centrifuge with F-45-30-11 rotor). D-glucose, ethanol and glycerol were enzymatically assayed using specific kits from Boehringer Mannheim (Indianapolis, IN, USA), following manufacturer instructions.

In situ assay of enzyme activities

Enzyme activities were determined *in situ* using *S. cerevisiae* permeabilized cells [36]. Permeabilization was achieved by incubation with 0.01% digitonin in 0.1 M Mes (pH 6.5) for 15 min at 30 °C and 160 r.p.m. in an orbital shaker incubator (Infors HT). Enzyme activities were determined at 30 °C in a 1.5 mL reaction volume. All assays were performed on a Beckman DU-7400 diode array spectrophotometer (Beckman-Coulter, Fullerton, CA, USA), with temperature control and magnetic stirring, essential to maintain isotropic conditions during the assay.

Enolase activity was followed by measuring phosphoenolpyruvate formation at 240 nm. The reaction mixture, containing 50 mM Tris/HCl (pH 7.4), 100 mM KCl, 1 mM $MgSO_4$, 0.01 mM EDTA and 0.5 μg of protein in permeabilized cells, was preincubated for 10 min, and the reaction was started by the addition of 4 mM 3-phosphoglycerate. In all assays, endogenous phosphoglycerate mutase activity was present in a large excess compared to enolase, and therefore the measured activity solely depends on enolase.

Sensitivity analysis

Modeling and computer simulation were used to evaluate the effects of enolase, aldolase and phosphoglycerate mutase activity changes on glycolytic flux, defined as the rate of ethanol formation. The effect of glycerol-3-phosphate dehydrogenase activity on the steady-state concentration of methylglyoxal was also investigated.

The kinetic model used in this study was based on the model of Hynne *et al*. [37], which includes most glycolytic enzymes, although the reactions of enolase and phosphoglycerate mutase are lumped together in an overall reaction. This model was extended to include these two reactions, with kinetic equations and parameters as in the model of Teusink *et al*. [38]. The connection with methylglyoxal metabolism was achieved by including the model of Gomes *et al*. [19], which comprises the glyoxalase pathway, aldose reductase and methylglyoxal formation from the triose phosphates. Simulations were performed with the software package POWER-LAW ANALYSIS AND SIMULATION, PLAS (A.E.N. Ferreira, Universidade de Lisboa, Portugal; http://www.dqb.fc μL.pt/docentes/aferreira/plas.html).

Protein structure

Enolase dimer structure was represented by PDB entry 1ebh, containing Mg. It has 95% identity and 4% homology with enolase 2. Molecular graphics images were produced using the UCSF CHIMERA package from the Resource for Biocomputing, Visualization, and Informatics at the University of California, San Francisco (supported by NIH P41 RR-01081) [39]. Relative solvent surface acessibility was calculated according to the method of Gerstein [40].

Acknowledgements

We thank Dr J. Prieto for providing the YEpGRE3 transformant, Dr H. M. Park for the gift of the yeast enolase polyclonal antibody and Dr K. Uchida for the gift of the argpyrimidine monoclonal antibody. We also acknowledge Dr R. Nagaraj for the gift of the methylglyoxal antibody and for fruitful discussions. We wish to acknowledge Ana Varela Coelho and Gonçalo Graça for providing data from the Laboratório de Espectrometria de Massa at the Instituto de Tecnologia Química e Biológica, Universidade Nova de Lisboa, Oeiras, Portugal. This work was supported by grants SFRH/BD/13884/2003 (RAG), SFRH/BD/23035/2005 (HVM) and POCTI/ESP/48272/2002 (MSS) from the Fundação para a Ciência e a Tecnologia, Ministério da Ciência e Tecnologia, Portugal.

References

1 Brownlee M (1995) Advanced protein glycosylation in diabetes and aging. *Annu Rev Med* **46**, 223–234.
2 Lyons TJ, Silvestri G, Dunn JA, Dyer DG & Baynes JW (1991) Role of glycation in modification of lens

crystallins in diabetic and nondiabetic senile cataracts. *Diabetes* **40**, 1010–1015.
3 Miyata T, van Ypersele de Strihou C, Kurokawa K & Baynes JW (1999) Alterations in nonenzymatic biochemistry in uremia: origin and significance of 'carbonyl stress' in long-term uremic complications. *Kidney Int* **55**, 389–399.
4 Kume S, Takeya M, Mori T, Araki N, Suzuki H, Horiuchi S, Kodama T, Miyauchi Y & Takahashi K (1995) Immunohistochemical and ultrastructural detection of advanced glycation end products in atherosclerotic lesions of human aorta with a novel specific monoclonal antibody. *Am J Pathol* **147**, 654–667.
5 Bucala R & Cerami A (1992) Advanced glycosylation: chemistry, biology, and implications for diabetes and aging. *Adv Pharmacol* **23**, 1–34.
6 Chen F, Wollmer MA, Hoerndli F, Munch G, Kuhla B, Rogaev EI, Tsolaki M, Papassotiropoulos A & Gotz J (2004) Role for glyoxalase I in Alzheimer's disease. *Proc Natl Acad Sci USA* **101**, 7687–7692.
7 Vitek MP, Bhattacharya K, Glendening JM, Stopa E, Vlassara H, Bucala R, Manogue K & Cerami A (1994) Advanced glycation end products contribute to amyloidosis in Alzheimer disease. *Proc Natl Acad Sci USA* **91**, 4766–4770.
8 Yan SD, Chen X, Schmidt AM, Brett J, Godman G, Zou YS, Scott CW, Caputo C, Frappier T & Smith MA (1994) Glycated tau protein in Alzheimer disease: a mechanism for induction of oxidant stress. *Proc Natl Acad Sci USA* **91**, 7787–7791.
9 Castellani R, Smith MA, Richey PL & Perry G (1996) Glycoxidation and oxidative stress in Parkinson disease and diffuse Lewy body disease. *Brain Res* **737**, 195–200.
10 Gomes R, Sousa Silva M, Quintas A, Cordeiro C, Freire A, Pereira P, Martins A, Monteiro E, Barroso E & Ponces Freire A (2005) Argpyrimidine, a methylglyoxal-derived advanced glycation end-product in familial amyloidotic polyneuropathy. *Biochem J* **385**, 339–345.
11 Richard JP (1993) Mechanism for the formation of methylglyoxal from triosephosphates. *Biochem Soc Trans* **21**, 549–553.
12 Booth AA, Khalifah RG, Todd P & Hudson BG (1997) In vitro kinetic studies of formation of antigenic advanced glycation end products (AGEs). Novel inhibition of post-Amadori glycation pathways. *J Biol Chem* **272**, 5430–5437.
13 Westwood ME & Thornalley PJ (1997) Glycation and Advanced glycation end-products. In *The Glycation Hypothesis of Atherosclerosis* (Colaco C, ed.), pp. 57–87. Springer Verlage, Heidelberg.
14 Shipanova IN, Glomb MA & Nagaraj RH (1997) Protein modification by methylglyoxal: chemical nature and synthetic mechanism of a major fluorescent adduct. *Arch Biochem Biophys* **344**, 29–36.
15 Ahmed MU, Brinkmann Frye E, Degenhardt TP, Thorpe SR & Baynes JW (1997) N-epsilon-(carboxyethyl) lysine, a product of the chemical modification of proteins by methylglyoxal, increases with age in human lens proteins. *Biochem J* **324**, 565–570.
16 Frye EB, Degenhardt TP, Thorpe SR & Baynes JW (1998) Role of the Maillard reaction in aging of tissue proteins. Advanced glycation end product-dependent increase in imidazolium cross-links in human lens proteins. *J Biol Chem* **273**, 18714–18719.
17 Racker E (1951) The mechanism of action of glyoxalase. *J Biol Chem* **190**, 685–696.
18 Vander Jagt DL & Hunsaker LA (2003) Methylglyoxal metabolism and diabetic complications: roles of aldose reductase, glyoxalase-I, betaine aldehyde dehydrogenase and 2-oxoaldehyde dehydrogenase. *Chem Biol Interact* **143–144**, 341–351.
19 Gomes RA, Sousa Silva M, Vicente Miranda H, Ferreira AE, Cordeiro CA & Ponces Freire A (2005) Protein glycation in *Saccharomyces cerevisiae*. Argpyrimidine formation and methylglyoxal catabolism. *FEBS J* **272**, 4521–4531.
20 Stromer T, Ehrnsperger M, Gaestel M & Buchner J (2003) Analysis of the interaction of small heat shock proteins with unfolding proteins. *J Biol Chem* **278**, 18015–18021.
21 Altenberg B & Greulich KO (2004) Genes of glycolysis are ubiquitously overexpressed in 24 cancer classes. *Genomics* **84**, 1014–1020.
22 Davidson SD, Cherry JP, Choudhury MS, Tazaki H, Mallouh C & Konno S (1999) Glyoxalase I activity in human prostate cancer: a potential marker and importance in chemotherapy. *J Urol* **161**, 690–691.
23 Di Ilio C, Angelucci S, Pennelli A, Zezza A, Tenaglia R & Sacchetta P (1995) Glyoxalase activities in tumor and non-tumor human urogenital tissues. *Cancer Lett* **96**, 189–193.
24 Merkulova T, Lucas M, Jabet C, Lamande N, Rouzeau JD, Gros F, Lazar M & Keller A (1997) Biochemical characterization of the mouse muscle-specific enolase: developmental changes in electrophoretic variants and selective binding to other proteins. *Biochem J* **323**, 791–800.
25 Speer O, Morkunaite-Haimi S, Liobikas J, Franck M, Hensbo L, Linder MD, Kinnunen PK, Wallimann T & Eriksson O (2003) Rapid suppression of mitochondrial permeability transition by methylglyoxal. Role of reversible arginine modification. *J Biol Chem* **278**, 34757–34763.
26 Lebioda L, Stec B & Brewer JM (1989) The structure of yeast enolase at 2.25-A resolution. An 8-fold beta + alpha-barrel with a novel beta beta alpha alpha (beta alpha) 6 topology. *J Biol Chem* **264**, 3685–3693.
27 Cohen R, Holland JP, Yokoi T & Holland MJ (1986) Identification of a regulatory region that mediates

glucose-dependent induction of the Saccharomyces cerevisiae enolase gene ENO2. *Mol Cell Biol* **6**, 2287–2297.
28 Ahmed N, Dobler D, Dean M & Thornalley PJ (2005) Peptide mapping identifies hotspot site of modification in human serum albumin by methylglyoxal involved in ligand binding and esterase activity. *J Biol Chem* **280**, 5724–5732.
29 Cashikar AG, Duennwald M & Lindquist SL (2005) A chaperone pathway in protein disaggregation. Hsp26 alters the nature of protein aggregates to facilitate reactivation by Hsp104. *J Biol Chem* **280**, 23869–23875.
30 Nagaraj RH, Oya-Ito T, Padayatti PS, Kumar R, Mehta S, West K, Levison B, Sun J, Crabb JW & Padival AK (2003) Enhancement of chaperone function of alpha-crystallin by methylglyoxal modification. *Biochemistry* **42**, 10746–10755.
31 Padival AK, Crabb JW & Nagaraj RH (2003) Methylglyoxal modifies heat shock protein 27 in glomerular mesangial cells. *FEBS Lett* **551**, 113–118.
32 Oya-Ito T, Liu BF & Nagaraj RH (2006) Effect of methylglyoxal modification and phosphorylation on the chaperone and anti-apoptotic properties of heat shock protein 27. *J Cell Biochem* **99**, 279–291.
33 Aguilera J & Prieto JA (2001) The Saccharomyces cerevisiae aldose reductase is implied in the metabolism of methylglyoxal in response to stress conditions. *Curr Genet* **39**, 273–283.
34 Pandey A, Andersen JS & Mann M (2000) Use of mass spectrometry to study signaling pathways. *Sci STKE 2000* **37**, plenary lecture number 1.
35 Gobom J, Nordhoff E, Mirgorodskaya E, Ekman R & Roepstorff P (1999) Sample purification and preparation technique based on nano-scale reversed-phase columns for the sensitive analysis of complex peptide mixtures by matrix-assisted laser desorption/ionization mass spectrometry. *J Mass Spectrom* **34**, 105–116.
36 Cordeiro C & Freire AP (1995) Digitonin permeabilization of Saccharomyces cerevisiae cells for *in situ* enzyme assay. *Anal Biochem* **229**, 145–148.
37 Hynne F, Dano S & Sorensen PG (2001) Full-scale model of glycolysis in Saccharomyces cerevisiae. *Biophys Chem* **94**, 121–163.
38 Teusink B, Passarge J, Reijenga CA, Esgalhado E, van der Weijden CC, Schepper M, Walsh MC, Bakker BM, Van Dam K, Westerhoff HV *et al.* (2000) Can yeast glycolysis be understood in terms of *in vitro* kinetics of the constituent enzymes? Testing biochemistry. *Eur J Biochem* **267**, 5313–5329.
39 Pettersen EF, Goddard TD, Huang CC, Couch GS, Greenblatt DM, Meng EC & Ferrin TE (2004) UCSF Chimera – a visualization system for exploratory research and analysis. *J Comput Chem* **25**, 1605–1612.
40 Gerstein M (1992) A resolution-sensitive procedure for comparing protein surfaces and its application to the comparison of antigen-combining sites. *Acta Cryst A* **48**, 271–276.